Journal of Materials and Environmental Sciences
ISSN : 2028-2508

JMES, 2017 Volume 8, Issue 10, Page 3747-3758

http://www.jmaterenvironsci.com/

Corrosion behavior of a smart inhibitor in hydrochloric Acid molar: Experimental and theoretical studies

R. Salim[1,2], A. Elaatiaoui[3], N. Benchat[3], E. Ech-chihbi[1,2], Z. Rais[2], H. Oudda[1] , F. El Hajjaji[2], Y. ElAoufir[1,4], M. Taleb[2]

[1] *Laboratory of separation processes, Faculty of Science, University Ibn Tofail, Kenitra, Morocco*
[2]*Laboratory of Engineering, Electrochemistry, Modeling and Environment (LIEME), Faculty of Sciences, University Sidi Mohamed Ben Abdellah, Fez, Morocco*
[3] *Laboratory of Applied Analytical Chemistry Materials and Environment (LCAAE), Faculty of sciences, University of Mohammed Premier, Oujda, Morocco*
[4]*Materials, Nanotechnology and Environment Laboratory, Faculty of Sciences, Rabat, Morocco*

Received 25 Feb 2017
Revised 1 June 2017
Accepted 3 June 2017

Keywords
- ✓ Inhibition,
- ✓ Imidazopyridine,
- ✓ C38,
- ✓ Efficiency,
- ✓ Adsorption,
- ✓ DFT,

salimrajae@gmail.com
Phone: +212665924696

Abstract

The corrosion inhibition of carbon steel C38 in 1 M HCl solution by a new synthesized compound of imidazopyridine namely **(2E)-3-[2-(4-chlorophenyl)imidazo[1,2-a]pyridin-3-yl]-1-(4 methoxy phenyl)prop-2-en-1-one**was studied using Tafel polarization, electrochemical impedance spectroscopy (EIS) and gravimetric measurements. The experimental results showed that the inhibition efficiency around 93% for 5.10^{-5}M at 303K. The thermodynamic and activation parameters for adsorption process were calculated. This compound was adsorbed according to the Langmuir isotherm and it's selected into a mixed-type. In other case a Quantum chemical parameters most calculated in corrosion inhibitor have been calculated and discussed. The quantum chemical calculations based on DFT methods at B3LYP / 6-31G (d,p) level of theory, were performed using Gaussian 09 program.

1. Introduction

The hydrochloric acid is one of the most acidic solutions using in chemical industrial processes because of their ability of picking, cleaning and descaling the metallic installation **[1-4]**. In order to reduce the damages caused by their application and protect these aspects a several research makes reposed by the addition of a molecular into the acidic solution which namely inhibitors **[5]**. The most inhibitors used today for corrosion effect is the organic ones because they containing heteroatom such as sulphur, phosphorus, nitrogen, oxygen which induce greater adsorption of these molecular onto the carbon steel surface **[6-10]**. Also when was had an aromatic ring and conjugate π double or triple bonds **[11-12]**. It's well known that the imidazopyridine is good inhibitors against corrosion beside pyrazole **[13-14]**, imidazole **[15-16]**, bipyrazole **[17-19]** derivatives. In other side it's very important using in pharmaceutical industry such as antiviral, anti-inflammatory, and antibacterial **[20]**. The aim of this present study is to investigate the inhibition of a new synthesized compound of imidazopyridine derivatives namely (2E)-3-[2-(4-chlorophenyl) imidazo[1,2-a]pyridin-3-yl]-1-(4-methoxyphenyl)prop-2-en-1-one on carbon steel corrosion in 1M HCl. This investigation was evaluated by weight loss measurement, electrochemical, scanning electron microscopy (SEM) and functional Theory (DFT) methods which have been applied to study the mechanism of steel corrosion inhibition of this organic compound in acidic medium.

2. Experimental method

2.1. Material preparation

The steel used in this study is a carbon steel containing (in wt %) 99.21 Fe, 0.38 Si, 0.21 C, 0.05 Mn, 0.05 S, 0.09 P and 0.01 Al. the hydrochloric solution acid 1M was prepared by dilution of analytical grade 37%.the

surface of the specimens employed was mechanically polished with different grade of emery paper from 180 to 1200, rinsing with double distilled water, degreasing in acetone and drying before being immersed in the acid solution.

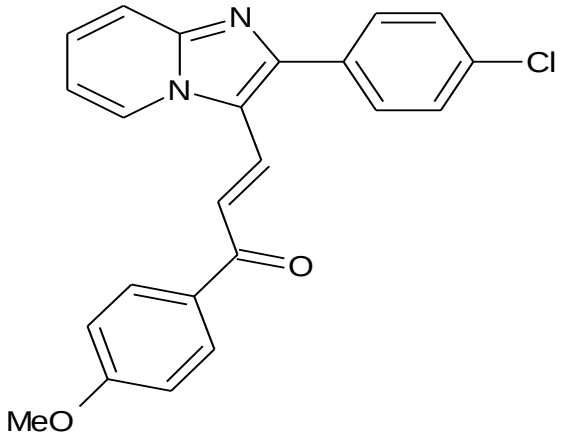

Fig.1. Chemical structures of organic compounds studied

2.2. Weight loss measurements

Weight loss experiments were carried out in a double-walled glass cell equipped with a thermostat cooling condenser at temperature of 303K in inhibited solution having a concentration from 5.10^{-5}M to 10^{-6}M.

2.3. Electrochemical test

The electrochemical experiment were performed by using a potentiostat Tacussel- Radiometer PGZ 100 and controlled by analysis software model Volta master 4. This method was carried out of a three electrode glass cell. The working electrode was the specimen used, the reference electrode was a saturated calomel electrode (SCEs) and the counter electrode was a platinum wire. The specimen was a square with exposed surface area 1 cm^2 which also ground with 1200 grit grinding papers, cleaned by distilled water, degreased with acetone and immersed in solution tested during 30 min until obtained the open circuit potential. The polarization curve was recorded from -700 to -200 mV/SCE with a scan rate of 1mV/s. The impedance spectroscopy measurements recorded at the open circuit potential in the frequency range from 100 KHz to 10 mHz. The result in this case is a semicircle spectra represented in the Nyquist diagram by using a transfer function analyses.

2.4. Computational method

The quantum chemical calculations were performed using DFT method which proved as a useful technique to check out the inhibitor/surface interaction and analyze the experiment data **[21]**. It's used the beck's three parameter exchange functional (B3LYP) **[22-23]**with a basis set of atomic orbital 6-31G(d) as implemented in Gaussian 03 program package **[24]**. The molecular properties estimated include the highest occupied molecular orbital (HOMO), lowest unoccupied molecular orbital (LUMO) and other molecular properties derived from HOMO and LUMO and their respective energies.

2.5. Scanning electron microscopic

The surface morphology of the steel samples in the absence and presence of our inhibitor was obtained after immersion time in 1 M HCl solution using SEM technique (model: JEOL, JSM 6400).

3. Results and discussion

3.1. Effect of concentration

3.1.1. Gravimetric measurement

The weight loss measurement of C38 steel in 1M HCl in the absence and the presence of various concentrations of inhibitor were determined after 6h of immersion at 303K. The values calculated of W_{corr} and the inhibition efficiency (IE %) determined by the following equations **[25]** :

$$W_{corr} = \frac{\Delta m}{S.t} \quad (1)$$

$$IE\% = \frac{W_{corr} - W'_{corr}}{W_{corr}} * 100 \quad (2)$$

Where W_{corr} and W'_{corr} are the corrosion rate of steel in the absence and presence of inhibitor, respectively.

Table 1. Corrosion rate of steel in 1M HCl with and without inhibitor at various concentrations and the corresponding inhibition efficiency

Medium	Concentration (M)	W_{corr} ($mg.cm^{-2}.h^{-1}$)	IE (%)
1M HCl	00	0,652	-
IPD	10^{-6}	0,143	**78,0**
	5.10^{-6}	0,079	**87,8**
	10^{-5}	0,049	**92,5**
	5.10^{-5}	0,042	**93,5**

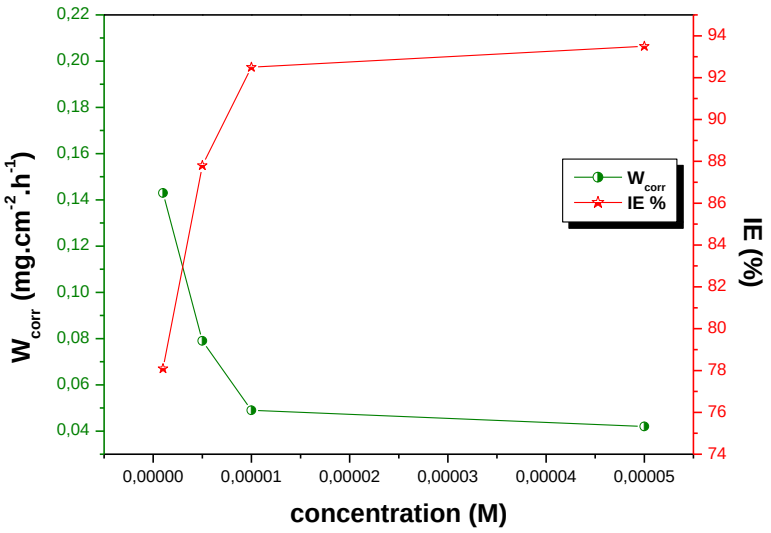

Fig.2. Variation of corrosion rate and inhibition efficiency with concentration of inhibitor

The corrosion parameters such as inhibition efficiency (IE) and corrosion rate (W_{corr}) at different concentration of inhibitor in 1M HCl at 303K are presented in table 1. As can be seen from table.1 and the fig. 2, the variation of inhibition efficiency are in opposite trend compared to the corrosion rate. In fact, the increase of IE is obtained up on addition of quite low concentrations of inhibitor and reaches the highest value to 93,5% at a concentration of 5.10^{-5}M. The corrosion inhibition can be attributed to the adsorption of IPD molecule at steel/ HCl solution interface **[26]**.

3.1.2. Polarization curve

The Potentiodynamic polarization curves of C38 steel in acid solution with and without concentrations of IPD are shown in Fig 3. The electrochemical parameters values of corrosion current densities (I_{corr}), corrosion potential (E_{corr}), cathodic Tafel slope (βc), and inhibition efficiency (IE %) of our molecular are regrouped in table 2.

In this case, the inhibition efficiency is defined as following equation:

$$IE\% = \frac{I_{corr} - I'_{corr}}{I_{corr}} * 100 \quad (3)$$

Where I_{corr} and I'_{corr} are the corrosion current density values in the absence and presence of inhibitor, respectively.

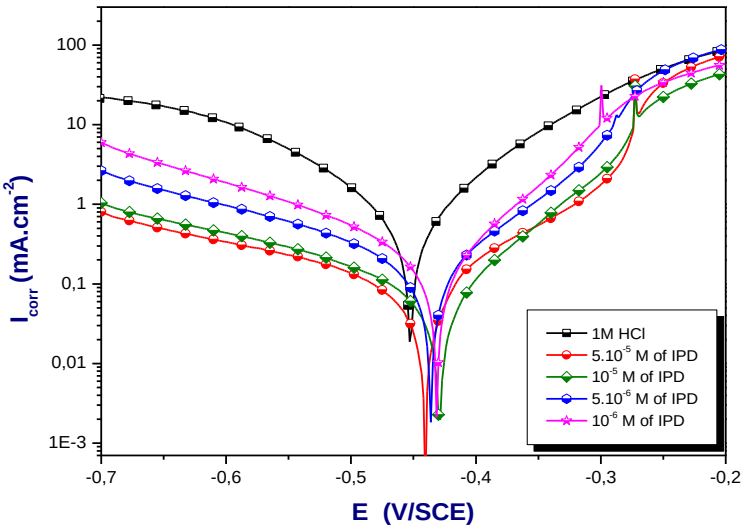

Fig.3. Polarization curve for carbon steel in 1 M HCl at different concentration of IPD

As can be seen from table 2 the current densities (I_{corr}) increase with decrease of inhibitor concentration, this increase leading to a decrease in the inhibition efficiency of our inhibitor. According to Alaoui et al and others authors **[27-28]**, when the displacement in potential is more than 85 mV/ E_{corr}, the inhibitor can be seen as an anodic or cathodic type, in case supposed as mixed type if the displacement in potential is less than 85 mV/ E_{corr}. In our study, the maximum displacement is less than 85 mV/ E_{corr}, which indicates that IPD acts as a mixed type inhibitor with predominant anodic. The results obtained by the potentiodynamic polarization curves confirm those obtained by weight loss measurements. The fig. 3 shows that potentials values higher than -350mV$_{ESC}$, the compound starts to be desorbed which reflect the formation of anodic protective films containing oxides.

Table 2. Potentiodynamic polarization parameters of the carbon steel in HCl without and with addition of IPD.

Medium	Concentration (M)	E_{corr} (mV/ECS)	I_{corr} (µA.cm^{-2})	-B_c (mV.dec^{-1})	IE%
1M HCl	00	-498	944	140	-
IPD	5.10^{-5}	-441	60	184	**93.6**
	10^{-5}	-429	67	165	**92.9**
	5.10^{-6}	-435	110	135	**88.3**
	10^{-6}	-430	203	119	**78.4**

3.1.3. Electrochemical impedance spectroscopy (EIS)

To complete our study, we imply the EIS method. The fig. 4 shows the Nyquist diagram in acid hydrochloric molar at 303K without and with various concentrations of synthesized inhibitor. The inhibition efficiency was calculated from following equation:

$$IE\% = \frac{R_{ct} - R'_{ct}}{R_{ct}} * 100 \qquad (4)$$

Where R_{ct} and R'_{ct} are respectively the charge transfer resistance in the absence and the presence of inhibitor.

The Nyquist plots are not perfect semicircles which can be attributed to the frequency dispersion as a result of the roughness and inhomogeneous of electrode surface **[29-30]**. Moreover, the diameter of the capacitive loop in the presence of inhibitor is bigger than the uninhibited solution and increase with inhibitor concentration. Therefore, a reduction in corrosion rate was observed. From the impedance data (table 3) we remarked that the value of R_{ct} increases with increasing of inhibitor concentration which indicates also an increase in the corrosion efficiency toattainmaximum value of 93.6% at 5.10^{-5}M. This percentage was according to a minimum value of surface heterogeneity which attributed to the adsorption of our compound. These results leading to suggest that a layer protective film was formed on the electrode surface.

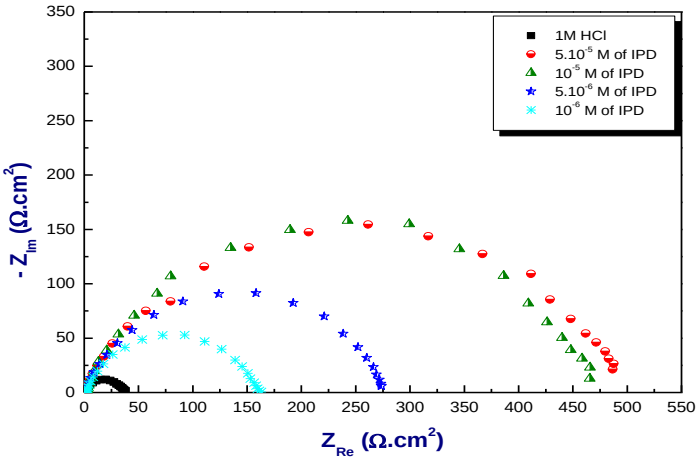

Fig.4. Impedance plots of carbon steel obtained in 1M HCl in the absence and presence of various concentrations of inhibitor.

The effective capacity C_{dl} can be calculated using the following mathematical formulas from the CPE:

$$C_{dl} = (Q * R_{tc}^{1-n})^{1/n} \quad (5)$$

Where Q is the constant phase angle (CPE) CPE constant, $R_{ct}$is the charge transfer resistance and n indicate the values of surface heterogeneity (0<n<1) **[31]**.

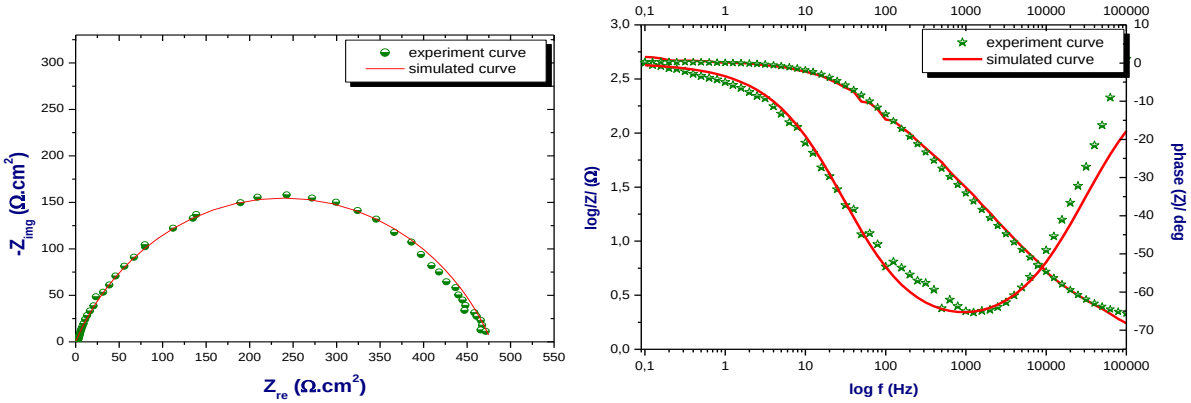

Fig.5. EIS Nyquist and bode diagrams for carbon steel/1M HCl + 5.10^{-5}M of IPD interface

Table 3. Impedance parameters of carbon steel in 1M HCl containing different concentrations of the studied compound.

Medium	Concentration (M)	R_s (Ω. cm^2)	R_{ct} ($\Omega.cm^2$)	Q ($\mu F.s^{n-1}$)	n	C_{dl} ($\mu F.cm^{-2}$)	IE%	Θ
1M HCl	00	1.123	35	315	0.770	121	--	--
IPD	5.10^{-5}	1.123	497	72.2	0.706	18.1	**93.0**	0.930
	10^{-5}	1.744	478	51.6	0.731	13.2	**92.7**	0.927
	5.10^{-6}	0.877	276	89.8	0.757	27.5	**87.3**	0.873
	10^{-6}	1.422	160	157	0.757	48.3	**78.2**	0.782

By fitting the experimental data of impedance of Nyquist representation, the equivalent circuit model obtained was presented in fig. 6, this circuit has a capacitance phase element Q which in parallel with charge transfer resistance R_{ct}. the both, Q and R_{ct} was in series with resistance solution R_s. As example the fitting of

experimental impedance and bode diagram for inhibited solution at optimum concentration are presented in fig. 5.

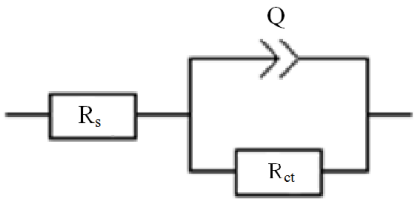

Fig.6. Equivalent electrical circuit model used to fit impedance spectra

3.1.4. Adsorption isotherm

In order to know more information about the interaction happens between the inhibitor and carbon steel surface we need to trace the adsorption isotherm. This isotherm depends on several parameters such as the nature and charge of the corroding metal, the inhibitor's chemical structure and the charge distribution in the inhibitor's molecule **[32].** For our inhibitor a several adsorption isotherm are assessed but the best fitted straight line is obtained from the plot of C_{inh}/θ versus C_{inh} with slopes around unity. As a result, we can say that IPD was obeyed to the Langmuir's adsorption isotherm by following equations:

$$\frac{C_{inh}}{\theta} = \frac{1}{K} + C_{inh} \quad (6)$$

$$K = \frac{1}{55.5} \exp\left(-\frac{\Delta_{ads}G^{\circ}}{RT}\right) \quad (7)$$

Where K is the adsorption-desorption equilibrium constant and ΔG^0_{ads} is the standard free energy of adsorption, 55.5 is a value of the molar concentration of water in the solution **[33]**.

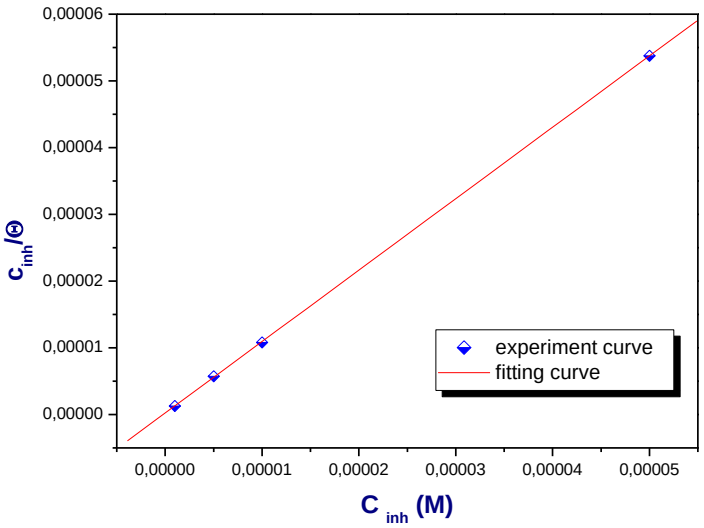

Fig.7. Langmuir adsorption isotherm of IPD on carbon steel surface in 1M HCl at 303 K

Table 4. Thermodynamic parameters for the adsorption of IPD onto the carbon steel surface in 1M HCl at 303K

Inhibitor	slope	K (M^{-1})	R^2	ΔG^0_{ads} ($KJ.mol^{-1}$)
IPD	1.07	$4.4.10^6$	0.999	-47.8

Table.4 regroups the values of equilibrium constant and free energy of adsorption. Literately, the ΔG^0_{ads} values of - 20 kJ mol^{-1}or less negative are associated with physisorption. While those of -40 kJ. mol^{-1}or higher involve

a strong interaction between the inhibitor molecule and the metal surface to form a coordinate covalent bond, chemisorption **[34-35].** It is show that the calculated ΔG^0_{ads} value is -47,3 kJ.mol^{-1}, indicating, therefore that the adsorption mechanism of the inhibitor tested on carbon steel surface in 1M HCl solution as typical of chemisorption **[36-37]** which possibly can be attributed to the donation π-electron by the aromatic rings, the nonbinding electron pair of two nitrogen of imidazopyridine derivative.

3.2. Effect of temperature

The temperature considered one of the parameters can change the interaction between carbon steel and acidic solution with or without inhibitor. In our study, the measurements are taken at range of temperature from 303 to 333K during 30min of immersion and the corresponding results regroups in table 5 and presented in fig. 8 which shows an increase of I_{corr} with increasing of temperature and it is more pronounced for inhibited solution. Also the slight variation in the inhibition efficiency with the rise of temperature indicates that the higher temperature does not a big influence on the adsorption of IPD on the metal surface.

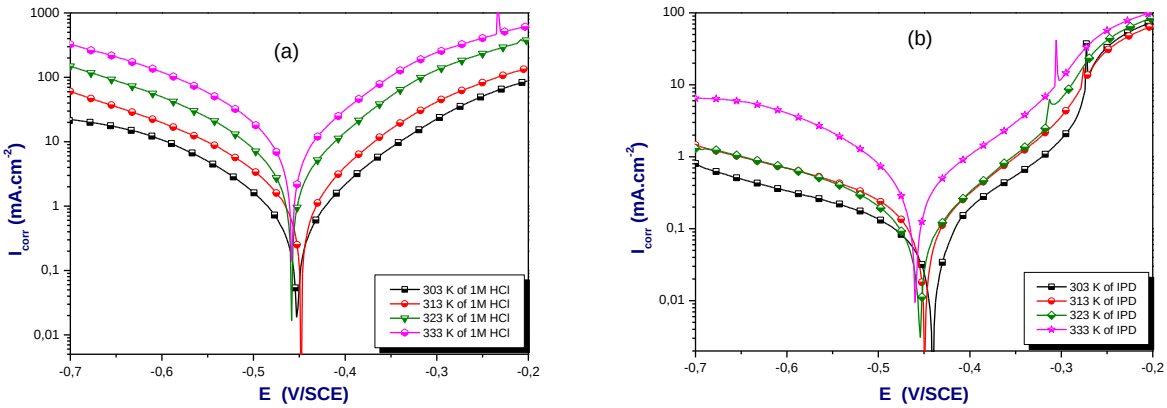

Fig.8. Effect of temperature on the behavior of carbon steel/1M HCl interface in (a) uninhibited solution, (b) at 5.10^{-5}M of IPD

Table 5. Influence of temperature on the corrosion rate and inhibition efficiency of carbon steel in 1 M HCl at different concentrations of IPD.

Medium	Temperature (K)	E (mV/ECS)	I_{corr} (µA.cm^{-2})	βc (mV.dec^{-1})	IE%
1M HCl	303	-453	944	-140	--------
	313	-451	1418	-119	--------
	323	-461	1962	-215	---------
	333	-460	2868	-205	---------
IPD	303	-441	60	-184	**93.6**
	313	-450	134	-132	**90.5**
	323	-454	272	-126	**86.1**
	333	-459	481	-99	**83.2**

In order to calculate activation parameters for the corrosion process, Arrhenius Eq. (9) and transition state Eq. (10) were used **[38-39]**:

$$I_{corr} = Ae^{\left(\frac{-Ea}{RT}\right)} \quad (9)$$

$$I_{corr} = \frac{RT}{Nh}\exp\left(\frac{\Delta S^*}{R}\right)\exp\left(-\frac{\Delta H^*}{RT}\right) \quad (10)$$

Where I_{corr} is the corrosion rate, R is the gas constant, T is the absolute temperature, A is the pre-exponential factor, h is the Plank's constant and N is Avogadro's number, Ea is the activation energy for corrosion process, ΔH* is the enthalpy of activation and ΔS* is the entropy of activation. The activation energy was determined

from the slopes of the weight loss (Ln I_{corr}) versus 1000/T, carbon steel in the corrosive medium with and without addition of inhibitor (Fig.9).

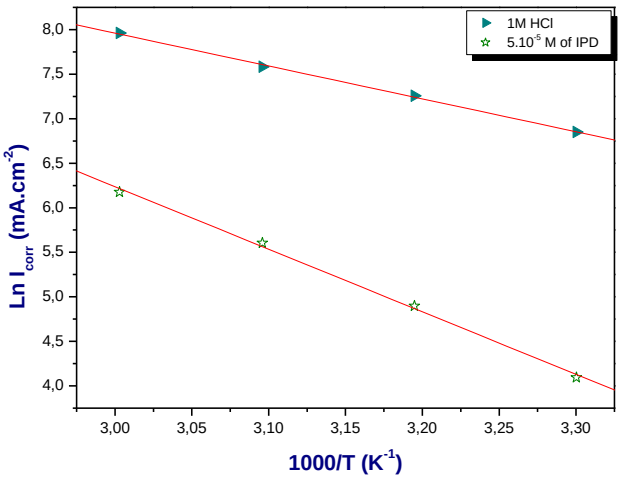

Fig.9. Arrhenius plots of carbon steel in 1M HCl at optimal concentration of IPD

As can be seen from the table 6, the values of Ea determined in inhibited solution are higher than uninhibited. This increasing of activation energy may be selected as physical adsorption that occurs in the first stage **[40]**.Ismaily Alaoui et al. **[41]** pointed out that when the activation energies increase, we can suggest that the mechanism of the corrosion process in inhibited solution modified also. Therefore, it's could be interpreted as the benzo-imidazopyridine adsorbed on steel surface by a physical (electrostatic) mechanism and form an adsorptive film **[42, 40]**.

In other hand, the values of enthalpy and entropy of activation determined from the plots of (Ln I_{corr}/T) versus 1000/T give a straight line with a slope of **ΔH*/R** and an intercept of **(ln(R/N.h)+ ΔS*/R** as shown in fig. 10.

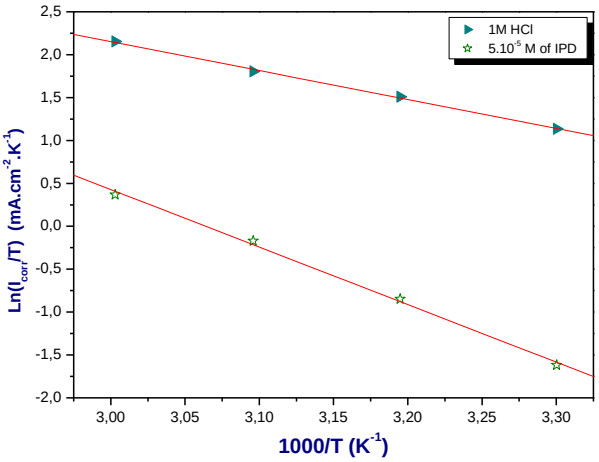

Fig.10. Arrhenius plots of LnW_{corr}/T versus 1000/T at optimal concentration of IPD

The table 6 shows that the ΔH* value for dissolution reaction of carbon steel is higher in the presence of IPD (55.8 kJ.mol^{-1}) than the uninhibited solution (14 kJ.mol^{-1}). The positive sign of the enthalpies ΔH* reflect the endothermic nature of the steel dissolution process which mean that the dissolution of carbon steel is more difficult **[43]**. Usually, the increase of ΔS* interpreted as an increase in disorder as the reactants are converted to the activated complexes **[44]**. Inspection of table 6, we note that a less negative value of ΔS* is calculated in the presence of IPD, while a more negative value is showed in uninhibited solution. This result interpreted as an increase in disorder **[40]**.

Table 6. Activation parameters of carbon steel dissolution in 1M HCl in the absence and in the presence of IPD.

Concentration (M)	Ea ($kJ.mol^{-1}$)	ΔH* ($kJ.mol^{-1}$)	ΔS* ($kJ.mol^{-1}.K^{-1}$)
1M HCl	30.7	28.0	-107.4
5.10^{-5} M of IPD	58.4	55.8	-38.5

3.3. Scanning electron microscopic (SEM)

The surface analysis is too important to know if our inhibitor adsorbed into specimen surface. SEM photographs were obtained after immersion of specimen surface in solution during 6h without and with the optimum concentration of inhibitor.The fig. 11indicates the finely polished characteristic surface of carbon steel although the presence of some scratches due to polishing (fig. 11-a) and the strongly damaged in the absence of inhibitor due to the direct attack of aggressive acids (fig. 11-b). By comparing to fig. 11-c appears that carbon steel surface is free from corrosion in HCl solution. This is due to the formation of an adsorbed film of inhibitor on the surface. This shows that the inhibitor inhibits corrosion of carbon steel in 1M HCl solution **[12,45]**.

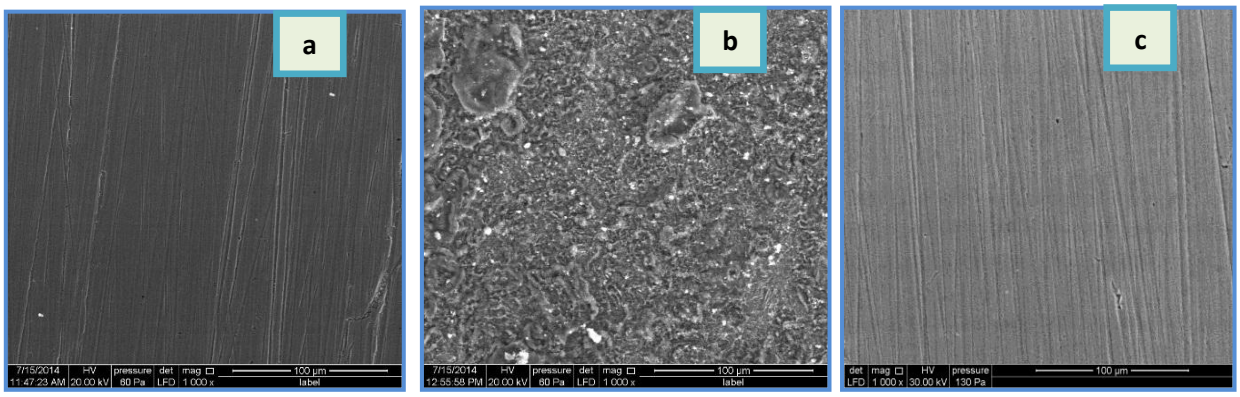

Fig.11. SEM image of carbon steel surface **(a)** before, **(b)** after 6 hours of immersion in 1M HCl solution and **(c)** in the presence of inhibitor (IPD)

3.4. Quantum chemical calculations

The calculations of quantum chemical are used to make sure the relationship between the inhibition effect of the synthesized inhibitor and its molecular structures. The optimized molecular structureand the frontier molecular orbitals density distributions are shown in fig. 12 and 13 respectively. The quantum chemical parameters are regrouped in table 7.

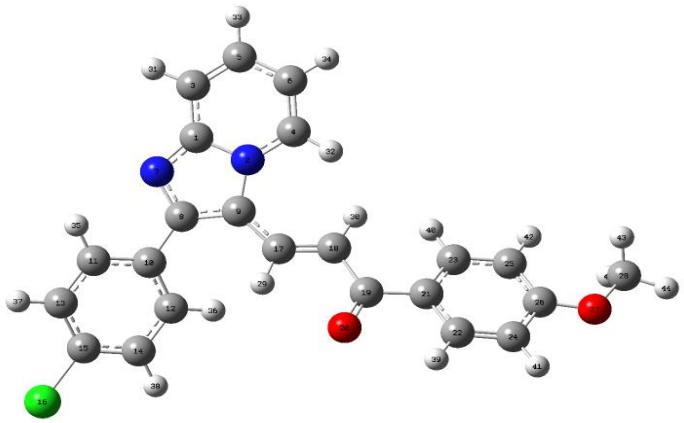

Fig.12. Optimized structure of studied molecule obtained by B3LYP/6-31G** level

As can be seen from fig. 13, the electron density of the HOMO and LUMO location was distributed almost of the entire molecule. E_{HOMO} is often associated with the ability of a molecule to donate electron. High value of E_{HOMO} may be shows a tendency of the molecule to donate electrons to appropriate acceptor molecules with low energy and empty molecular orbital**[46]**.

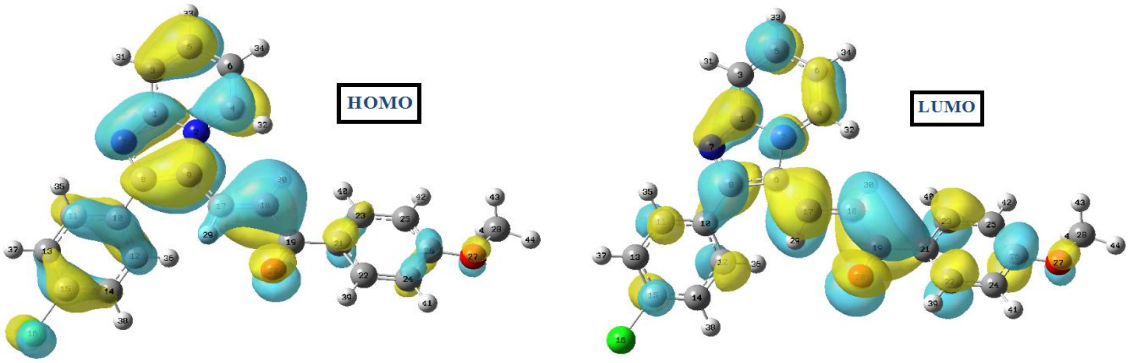

Fig.13. Frontier molecule orbitals density distributions of the synthesized inhibitor

in other case, E_{LUMO} indicate the capacity of the molecule to accept electrons and when the value of E_{LUMO} get more lower, the probability of molecular to accept electrons is elevate **[47]**.According to the frontier orbitals theory, the reaction of reactants mainly occurs on HOMO and LUMO. So the smaller gap (ΔE) between E_{HOMO} and E_{LUMO} is the more probable to donate and accept electrons.Thevalue of ΔE (table 7) suggesting the strongest ability of our inhibitor to form coordinate bonds with d-orbital of metal **[48]**.Additionally, when the value of dipole moment (μ) is higher, we can see an increasing of corrosion inhibition **[49]** which is the same of our case because the value of μ is important. This value shows agreement with the experimental results mentioned above.

Table 7. Quantum chemical parameters of IPD

Quantum parameters	Values
E_{HOMO} (eV)	-5.664
E_{LUMO} (eV)	-2.049
ΔE (eV)	3.614
A (eV)	2.049
I (eV)	5.664
χ(eV)	3.857
Ƞ (eV)	1.807
μ (Debey)	7.884
ΔN	0.869

According to Koopman's theorem **[50]**, the energies of HOMO and LUMO are correlated to the ionization potential (I) and the electron affinity (A), respectively which defined as follows:

$$I = -E_{HOMO} \quad (11) \qquad A = -E_{LUMO} \quad (12)$$

The energy gap is determined as follow:

$$\Delta E = E_{LUMO} - E_{HOMO} \quad (13)$$

The values of I and A were considered for the calculation of the electronegativity χ and the global hardness η was determined using the following equations:

$$\chi = 1/2(I + A) \quad (14)$$

$$\eta = 1/2(I - A) \quad (15)$$

The fraction of electrons transferred from inhibitor to metal surface (ΔN) was estimated according to Pearson **[51]**.

$$\Delta N = \frac{\chi_{Fe} - \chi_{inh}}{2(\eta_{Fe} - \eta_{inh})} \quad (16)$$

Where a theoretical value for the electronegativity of bulk iron was used, χ(Fe) = 7eV, and a global hardness of η (Fe) = 0 was used **[52]**.

Generally, the inhibition efficiency increases with the increase in electron-donating ability to the metal surface. According to Lukovits's study, this is true if $\Delta N < 3{,}6$ **[46]**. Based on these calculations, we can say that our inhibitor has a favors chemical adsorption on the steel surface.

Conclusion

The results obtained show that our compound is a good inhibitor of carbon steel in 1M HCl.

- The inhibition efficiency of IPD increased with inhibitor concentration.
- The Potentiodynamic polarization measurements show that IPD act as mixed-type inhibitor with anodic predominance at 5.10^{-5}M.
- EIS measurement results indicate that the charge transfer resistance increases greatly and its capacitance decreases by increasing the inhibitor concentration.
- The weight loss, electrochemical impedance spectroscopy and polarization curves were in good agreement.
- The adsorption of IPD on the carbon steel surface follows the Langmuir adsorption isotherm.
- The results obtained from thermodynamic parameters activation and adsorption process indicate that IPD adsorbed by mixed type physisorption and chemisorption.
- The scanning electron microscopy shows a smoother surface for inhibited metal sample than uninhibited samples due to the formation of film like deposit on the inhibited surface.
- The results of quantum chemical calculations using DFT method are in good agreement with the experimental investigations

References

1. Al Hamzi A.H., Zarrok H., Zarrouk A., Salghi R., Hammouti B., Al-Deyab S.S., Bouachrine M., Amine A., Guenoun F., *Intern. J. ELectrochem. Sci.*, 8 (2), (2013) 2586-2605.
2. AitAlbrimi Y., AitAddi A., Douch J., Hamdani1 M., Souto R.M., *Int. J. Electrochem. Sci.*, 11 (2016) 385 – 397
3. Shahabi S., Norouzi P., Ganjali M.R., *Int. J. Electrochem. Sci.*, 10 (2015) 2646 – 2662
4. Bommersbach P., Alemany-Dumont C., Millet J.P., Normand B., *Electrochim. Acta* 51 (2005) 1076–1084.
5. Dahmani M., Et-Touhami A., Al-Deyab S.S., Hammouti B., Bouyanzer A., *Int. J. Electrochem. Sci.*, 5 (2010) 1060.
6. Ben Aoun S., *Der Pharma Chemica*, 5(3) (2013) 294-304
7. Zerga B., Attayibat A., Sfaira M., Taleb M., Hammouti B., EbnTouhami M., Radi S., Rais Z., *J. Appl. Electrochem.* 40 (2010) 1575
8. Ben Hmamou D., Zarrouk A., Salghi R., Zarrok H., EbensoEno E., Hammouti B., Kabanda M. M., Benchat N., Benali O., *Int. J. Electrochem. Sci.*, 9 (2014) 120 – 138
9. Belayachi M., Serrar H., Zarrok H., El Assyry A., Zarrouk A., Oudda H., Boukhris S., Hammouti B., EbensoEno E., Geunbour A., *Int. J. Electrochem. Sci.*, 10 (2015) 3010 –
10. Herrag L., Hammouti B., Elkadiri S., Aouniti A., Jama C., Vezin H., Bentiss F., *Corros. Sci.* 52 (2010) 3042.
11. Zarrouk A., Hammouti B., Zarrok H., Bouachrine M., Khaled K.F., Al-Deyab S.S., *Int. J. Electrochem. Sci*, 7 (2012) 89.
12. El Arrouji S., Ismaily Alaoui K., Zerrouki A., EL Kadiri S., Touzani R., Rais Z., Filali Baba M., Taleb M., El-Hajjaji F., Chetouani A., Aouniti A., *J. Mater. Environ. Sci*, 2016, 7(1), 299-309.
13. Abdallah M., El Naggar M.M., *Mater. Chem. Phys.* 71 (2001) 291.
14. Benabdellah M., Yahyi A., Dafali A., Aouniti A., Hammouti B., Ettouhami A. *Arab. J. Chem*, 2011, 4, 343.
15. Abdallah M., Megahed H.E., Sobhi M., *Monatshefte fur Chem.* 141, 1287 (2010)
16. Mousavi M., Mohammadalizadeh M., Khosravan A., *Corros. Sci.* 53, 3086 (2011)
17. Tebbji K., Oudda H., Hammouti B., Benkaddour M., El Kodadi M., Malek F., Ramdani A., *Appl. Surf. Sci.* 241 (2005) 326.
18. Touhami F., Aouniti A., Kertit S., Abed Y., Hammouti B., Ramdani A., El Kacemi K., *Corros. Sci.* 42 (2000) 929.
19. Dafali A., Hammouti B., Touzani R., Kertit S., Ramdani A., El Kacemi K., *Anti Corros. Meth. Mater*. 49 (2002) 96.

20. Elaatiaoui A., Rokni Y., Mohammed K., Asehraou A., Chelfi T., Saddik R., Oussaid A., Villalgordo J.M., Abouricha S., El Mahi B., Oussaid A., Zarrouk A., Benchat N.,*J. Mater. Environ. Sci.* 6 (2015) 2083-2088
21. Obi-Egbedi N.O., Obot I.B., El-Khaiary M.I., *J. Mol.Struct*, 1002 (2011) 86-96
22. Lee C., Yang W., Parr R.G., *Phys. Rev.* B, 37 (1988) 785-789
23. Becke A.D., *J. Chem. Phys*, 98 (1993) 1372-1377
24. Frisch M.J., Trucks G.W., Schlegel H.B., Scuseria G.E., Robb M.A., Gaussian Inc., Wallingford CT (2004)
25. Scendo M., *Corros. Sci.* 50 (2008) 1584.
26. Khaled K.F., *Mater. Chem. Phys.* 125 (2011) 427.
27. Alaoui K., El Kacimi Y., Galai M., Touir R., Dahmani K., Harfi A., EbnTouhami M., *J. Mater. Environ. Sci.* 7 (7) (2016) 2389-2403
28. Quraishi M.A., Ahmad S., Venkatachari G., *Bull. Electrochem.*,12 (1996) 109.
29. Bouyanzer A., Hammouti B., Majidi L. Mat. Lett., 2006, 60, 2840.
30. Bousskri A., Anejjar A., Salghi R., Jodeh S., Touzani R., Bazzi L., Lgaz H., *J. Mater. Environ. Sci.* 7 (11) (2016) 4269-4289
31. Lopez D.A., Simison S.N., de Sanchez S.R., *Electrochim. Acta*, 48 (2003) 845–854.
32. Ghazoui A., Saddik R., Benchat N., Hammouti B., Guenbour M., Zarrouk A., Ramdani M. *Der Pharma Chemica*, 4 (1) (2012) 352-364
33. Cano E., Polo J.L., La Iglesia A., Bastidas J.M., *Adsorption*, 10 (2004) 219-225.
34. Ghazoui A., Benchat N., El-Hajjaji F., Taleb M., Rais Z., Saddik R., Elaatiaoui A., Hammouti B., *Journal of Alloys and Compounds* 693 (2017) 510e517
35. El Ouasif L., Merimi I., Zarrok H., El ghoul M., Achour R., Guenbour M., Oudda H., El-Hajjaji F., Hammouti B. J. Mater. Environ. Sci. 7 (8) (2016) 2718-2730
36. BhanVerma C., Quraishi M.A., Ebenso E.E., *Int. J. Electrochem. Sci.*, 9 **(2014)** 5507 - 5519
37. Benhiba F., Zarrok H., Elmidaoui A., El Hezzat M., Touir R., Guenbour A., Zarrouk A., Boukhris S., Oudda H., J. Mater. Environ. Sci. 6 (8) (2015) 2301-2314
38. Bockris J.O'M., Reddy A.K.N., Modern Electrochemistry, vol. 2, Plenum Press, New York, 1977.
39. Afia L., Salghi R., EbensoEno. E., Messali M., Al-Deyab S. S., Hammouti B. Int. J. Electrochem. Sci., 9 (2014) 5479 – 5495
40. EL Aoufir Y., Lgaz H., Bourazmi H., Kerroum Y., Ramli Y., Guenbour A., Salghi R., El-Hajjaji F., Hammouti B., Oudda H., *J. Mater. Environ. Sci.* 7 (12) (2016) 4330-4347
41. Ismaily A.K., Ouazzani F., kandrirodi Y., Azaroual A.M., Rais Z., Filali Baba M., Taleb M., Chetouani A., Aouniti A., Hammouti B., *J. Mater. Environ. Sci.* 7 (1) (2016) 244-258
42. Ech-chihbi E., Salim R., Oudda H., Elaatiaoui A., Rais Z., Oussaid A.,ElHajjaji F., Hammouti B., Elmsellem H.,Taleb M., *Der Pharma Chemica*, 8(13) (2016) 214-230
43. Lgaz H., Salghi R., Larouj M., Elfaydy M., Jodeh S., Rouifi Z., Lakhrissi B., Oudda H., *J. Mater. Environ. Sci.* 7 (12) (2016) 4471-4488
44. El Ouali I., Hammouti B., Aouniti A., Ramli Y., Azougagh M., Essassi E.M., Bouachrine M., *J. Mater Environ. Sci.* 1 (2010) 1–8.
45. Salim R., EchChihbi E., Oudda H., ELAoufir Y., El-Hajjaji F., Elaatiaoui A., Oussaid A., Hammouti B., Elmsellem H. Taleb M., *Der Pharma Chemica*, 8(13) (2016) 200-213
46. Ben Hmamou D., Salghi R., Zarrouk A., Zarrok H., Hammouti B., Al-Deyab S. S., El Assyry A., Benchat N., Bouachrine M., *Int. J. Electrochem. Sci.*, 8 (2013) 11526 - 11545
47. Ibrahim M.M., Amin M.A., Ichikawa K. J. Mol. Struct. 985 (2011) 191.
48. El Adnani Z., Mcharfi M., Sfaira M., Benzakour M., Benjelloun A.T., EbnTouhami M., Hammouti B., Taleb M. Int. J. Electrochem. Sci., 7 (2012) 6738 – 6751
49. Shahabi S., Norouzi P., Ganjali M. R., *Int. J. Electrochem. Sci.*, 10 **(2015)** 2646 - 2662
50. El Adnani Z., Mcharfi M., Sfaira M., Benjelloun A.T., benzakour M., EbnTouhami M., Hammouti B., Taleb M. Int. J. Electrochem. Sci., 7 (2012) 3982 – 3996
51. Ismaily A.K, El Hajjaji F., Azaroual M.A., Taleb M., Chetouani A., Hammouti B., Abrigach F., Khoutoul M., Abboud Y.,Aouniti A., Touzani R. *Journal of CPR*, 2014, 6(7):63-81
52. Arslan T., Kandemirli F., Ebenso E.E., Love I., Alemu H., *Corros. Sci.*, 51 (2009) 35.